

DESIGN OF NEW ANTI-BUCKLING FIXTURE FOR CYCLIC TENSION-COMPRESSION TESTING OF SHEET METAL

Jemal Ebrahim 

PhD student, Institute of Materials Science & Technology, Faculty of Mechanical Engineering
3515 Miskolc-Egyetemváros, e-mail: metjemal@uni-miskolc.hu

Zsolt Lukács 

PhD, Associate professor Institute of Materials Science & Technology, Faculty of Mechanical Engineering
3515 Miskolc-Egyetemváros, e-mail: zsolt.lukacs@uni-miskolc.hu

Abstract

The currently available anti-buckling fixtures for uniaxial tension-compression testing of sheet metal could not fulfill the requirements and standards. In this study, a unique system of the anti-buckling fixtures to enable getting accurate and repeatable isotropic and kinematic behavior of sheet metal was designed. The front surface of the specimen was fully supported during the initial position, tension, and compression and free from any buckling. Because using acrylic blocks, has a greater level of optical clarity, there was the possibility to measure the deformation on the front surface of the specimen using a digital image correlation system. The special pusher vice with compressed spring was attached to the fixture to avoid misalignment and calculating supplementary forces related to uniaxial direction. Furthermore, the new fixture was simple, flexible, and suitable for any universal testing machine.

Keywords: anti-buckling fixture, tension-compression testing, acrylic blocks, digital image correlation

1. Introduction

The sheet metal stamping process is the workhorse of automotive manufacturing. It is the dominant technique because of its low cost, involves a very high production rate, allows for producing very high complex features, and is compatible with the new generation of aluminum alloys. Of course, a small percentage of automotive bodies are made using the casting and extrusion process. *Figure 1* shows the general process to manufacture automotive components.

In recent years, the drive towards designing and manufacturing energy-efficient vehicles has propelled the automotive industry towards light-weighting with advanced materials, including high-strength aluminum alloys (HSAA) and advanced high-strength steels (AHSS) exhibiting high strength and ductility (Agha and Abu-Farha, 2022). Nowadays, non-heat-treatable AA5xxx and heat-treatable AA6xxx are popular candidates for automotive and aircraft industries, because they enable reduction of car body or an increase in fuel efficiency compared to parts made of steel (Choi et al., 2020).

Technical challenges in cold sheet metal stamping HSAA are wrinkling, splitting, and springback as shown in *Figure 2*. Wrinkling and splitting are visible challenges and very clear problems that can be addressed during the production process. However, springback is an invisible problem. It is usually the deviation from the intended shape from the stamped part and it will be warpage, distortion, or a combination of the two.

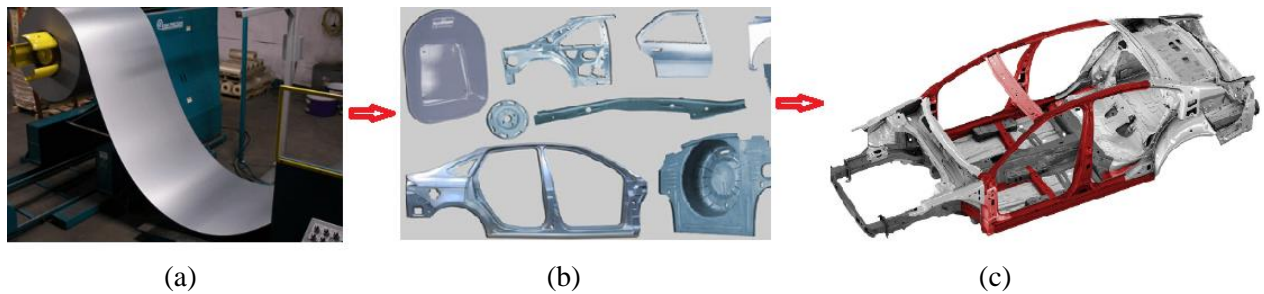


Figure 1. Manufacturing automotive components: (a) coil feeding; (b) stamped component; (c) assembly

Springback is related to the loading and unloading curve of the material. It is the amount of recovery after reaching the maximum load and going back to zero loads. Springback magnitude is directly proportional to the ratio of flow stresses to Young's modulus; this makes it typically high for such high-strength materials (Wagoner et al., 2013). Therefore, springback is highly dependent on material properties such as elastic modulus, Poisson's ratio, strain-hardening exponent, yield strength, or material anisotropy (Wagoner et al., 2013; Nanu and Brabie, 2012). For springback analysis, modeling the Bauschinger effect and cyclic hardening characteristics of materials is critical (Uemori et al., 1998). Determination of the stress-strain in uniaxial tension-compression loading for modeling of large-strain cyclic plasticity of sheet metals is therefore essential. The cyclic loading research of sheet metals is much more difficult. Because the sheet is prone to buckling in compression, the installation of a preventive fixture is needed on both sides of the sheet.

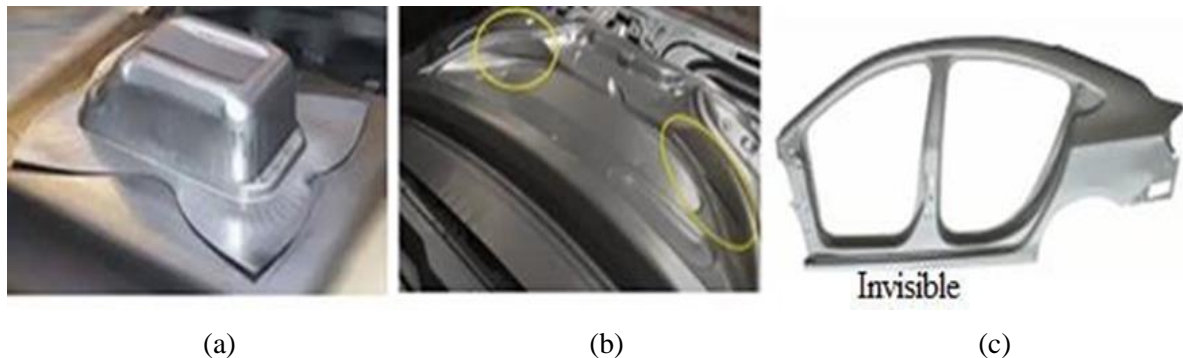


Figure 2. Different technical challenges in sheet metal stamping process: (a) wrinkles; (b) splits; (c) springback

Yoshida et al. (Yoshida et al., 2002) conducted a ~8% maximum cyclic strain acyclic test of bonded multiple mild and high strength steel specimens to overcome buckling. In the study, a unique device (specimen holder) for preventing buckling was attached to the specimen by coil springs and used a clip-on extensometer for strain measurements. Teflon sheets coated with petroleum jelly (vaseline) were put in their interfaces to reduce friction. The effect of pressure on the determination of stress-strain responses was negligible because of the lower pressure on the surface of the specimen. Cao et al. (Cao et al., 2009) developed a double-wedge setup to provide side force using six screws and prevent buckling in the specimen. Moreover, strain measurement was done by a laser extensometer with extended fins. The

setup was used to test dual-phase steel and precipitate hardened AA6xxx series sheets to achieve compressive strains of up to ~10%. Two upper and lower wedge-shaped plates cover the entire specimen on both sides. The upper wedge plates can slide against each other on the pockets machined on the middle wedge surface of the lower plate. A spring under tension is installed on each side of the device to ensure the alignment and keep the mating surface during testing. M Härtel et al. (Härtel et al., 2016) developed a new experimental setup for cyclic testing to meet some standards. The setup consists of clamps and of four moveable comb-shaped parts installed between a die set that is adapted to fit into a universal testing machine. A standardized specimen is placed between the two front parts and the two back parts. The comb-shaped clamps prevent buckling. A digital image correlation (DIC) system is used to measure strain on the thickness of the specimen. Indirect supplementary analysis was performed to account for the effect of side force and friction. Y. Chang et al. (Chang et al., 2020) introduced a new cyclic tensile-compressive fixture attachable to the universal tensile testing machine. The fixture had lower and upper segments connected with the force sensor and the worktable of the testing machine respectively. There were two T-shaped solid plates used to support the specimen which was covered by Teflon. Linear bearings are placed on the outer surface of the T-shaped plates to reduce the clamping friction between the supporting plates and the body of fixtures. Seven locking screws were used to fix the specimen in both the upper and lower part of the fixture. The two T-shaped solid plates had opposite movements to each other and used a modified extensometer to measure and monitor the strain. Z. Lukács et al. (Tisza and Lukács, 2014) introduced a new anti-buckling system to overcome the limitations experienced in former cyclic testing procedures. During the design of this device, the loading cycles should be done as a continuous tension-compression cycle which can be performed on a uniaxial testing machine applying a conventional extensometer for strain measurement. When the support constraint becomes excessive, the specimen would also be barreled and not completely free from buckling especially during expanding support plates.

But all the above-reviewed literature or previously designed anti-buckling fixtures are not completely cover the front surface of the specimen except for the fixture it was developed by Cao et al. (Cao et al., 2009). Therefore, all were not free from buckling during the compression test and considered measuring the deformation on the thickness of the specimen. All needs calculating supplementary side force, friction force, and other auxiliary forces like tension-compression of springs which has a direct relation with the uniaxial direction of tension-compression load using either theoretically or numerically. This work tries to shed some limitations on this topic by introducing a new anti-buckling device that is particularly designed to enable accurate and repeatable compression and cyclic testing.

2. Theoretical modelling of springback

The literature has described a number of techniques for measuring large-strain cyclic plastic deformation, however, there are important variations in the range of the strains and the stress-strain state. As a general requirement, it can be said that those test settings are the most advantageous when the stress and strain states are more uniform after analyzing the numerous applicable methodologies. To minimize measuring errors, it is also crucial to understand the material properties that characterize cyclic plastic deformation across a large range.

Material characteristics like elastic modulus, Poisson's ratio, strain-hardening exponent, yield strength, or material anisotropy have a significant impact on springback. Analyzing the stress-strain behavior of sheet metals during loading and unloading is vitally necessary for a more accurate simulation of springback phenomena (i.e. reverse loading). Numerous studies have been conducted to examine the

so-called cyclic plasticity. Previously, they were primarily concerned with low-cycle fatigue, therefore experiments were limited to minor plastic deformation. However, considerable work has lately been put into determining how the Bauschinger effect affects the cyclic behavior of sheet metallic materials under enormous strain (Yoshida and Uemori, 2002).

Two separate occurrences of stress-strain reactions define the Bauschinger effect. The two are the so-called “permanent softening” that develops after the transient period and the so-called “transient softening”, which is the smooth transient stress-strain response at the early stage of stress reversal. It is crucial to model the Bauschinger effect and cyclic hardening properties of materials. It is a suitable constitutive model for cyclic plasticity at large strain. Yoshida-Uemori is the material hardening model that is most frequently used to determine the performance of the springback.

The bounding surface and the motion of the yield surface within the bounding surface under uniaxial forward-reverse deformation are shown in *Figure 3* (Yoshida and Uemori, 2002).

2.1. Constitutive modeling

With the assumption of a small elastic and large plastic deformation, the rate of deformation \mathbf{D} is decomposed as:

$$\mathbf{D} = \mathbf{D}^e + \mathbf{D}^p \quad (1)$$

where \mathbf{D}^e and \mathbf{D}^p are the elastic and plastic parts of the rate, respectively. The decomposition of the continuum spin \mathbf{W} is given by:

$$\mathbf{W} = \mathbf{\Omega} + \mathbf{W}^p \quad (2)$$

where \mathbf{W}^p denotes the plastic spin and $\mathbf{\Omega}$ is the spin of substructures. The constitutive equation of elasticity is expressed by the equation:

$$\overset{\circ}{\boldsymbol{\sigma}} = \dot{\boldsymbol{\sigma}} - \mathbf{\Omega}\boldsymbol{\sigma} + \boldsymbol{\sigma}\mathbf{\Omega} = \mathbf{C}:\mathbf{D}^e \quad (3)$$

where $\boldsymbol{\sigma}$ and $\overset{\circ}{\boldsymbol{\sigma}}$ are the Cauchy stress and its objective rate, and $\mathbf{\Omega}$ is the elasticity modulus tensor. Here, (\circ) stands for the objective rate.

The present constitutive model of plasticity has been constructed within the framework of well-known two-surface modeling, wherein the yield surface moves kinematically within a bounding surface. Based on the von Mises criterion, the yield function f and the associated flow rule are given by the equations:

$$f = \frac{3}{2}(\mathbf{s} - \boldsymbol{\alpha}):(\mathbf{s} - \boldsymbol{\alpha}) - Y^2 = 0 \quad (4a)$$

$$\mathbf{D}^p = \frac{\partial f}{\partial \mathbf{s}} \dot{\lambda} \quad (4b)$$

where \mathbf{s} and $\boldsymbol{\alpha}$ denote the Cauchy stress deviator and the back stress deviator, respectively, and Y is the radius of the yield surface in the deviatoric stress space.

The bounding surface F is expressed by the equation:

$$F = \frac{3}{2}(\mathbf{s} - \boldsymbol{\beta}):(\mathbf{s} - \boldsymbol{\beta}) - (B + R)^2 = 0 \quad (5)$$

where β denotes the center of the bounding surface, and B and R are its initial size and isotropic hardening components.

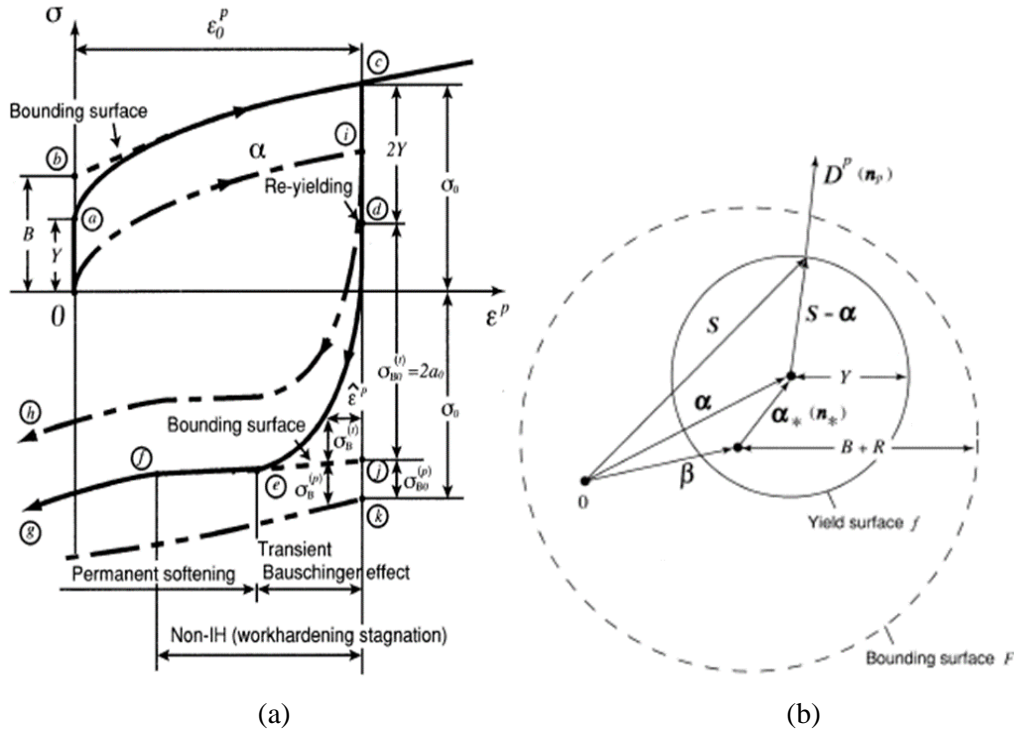


Figure 3. (a) The motion of the yield surface; (b) Bounding surface mixed isotropic-kinematic hardening

The transient Bauschinger deformation, which is characterized by early re-yielding and the subsequent rapid change in work-hardening rate, is described by the kinematic hardening of the yield surface. This deformation is primarily caused by the motion of less stable dislocations, such as piled-up dislocations. The global work-hardening, which is linked to the emergence of stable dislocation structures like cell walls, is represented by the isotropic hardening of the boundary surface. The disintegration of dislocation cell walls during forward deformation and the creation of new dislocation microstructures during reverse deformation is what lead to the permanent softening and work-hardening standstill. The kinematic hardening and non-isotropic hardening zones during stress reversals are assumed for the bounding surface in order to define such deformation properties under stress reversals.

A similar but rather practical approach is implemented in the AutoForm FEM package. The main idea of the AutoForm model is to use the same developing equations to describe the early re-plastification (early yielding) and the transient softening.

To implemented in the Auto Form finite element analysis material card, the reduction of the tangent modulus may be expressed as:

$$E_t = E_0[1 - \gamma(1 - e^{\chi p})] \quad (6)$$

where E_0 is the initial tangent modulus at zero plastic strain (i.e. Young's modulus), E_l is deformation-dependent tangential modulus, γ is a material parameter called young's reduction factor to express the reduction of the initial tangent modulus and χ is saturation constant.

The total reverse strain may be represented as the sum of a linear reverse strain and a non-linear reverse strain in order to generate the expression representing the aforementioned "smooth function". The linear reverse strain that defines the early re-yielding phase can be translated into an initial tangent modulus.

The non-linear reverse strain is approximated with an inverse hyperbolic tangent function and for the sum of linear and non-linear reverse strain the following expression can be written:

$$\varepsilon_r = \varepsilon_{rl} + \varepsilon_{rn} = \frac{\sigma_r}{E_1(p)} + K \operatorname{arctanh}^2 \left(\frac{\sigma_r}{2\sigma_h(p)} \right)^2 \quad (7)$$

where $\sigma_h(p)$ is the isotropic stress depending on the reverse plastic strain and K is a material parameter representing a typical strain distance affecting the steepness of the reverse stress curve (σ_r). ε_r is total reverse strain, ε_{rl} is linear reverse strain, ε_{rn} is non linear reverse strain.

Tangent modulus and the total reverse strain depend on three material parameters, i.e., γ , χ , and K . They will play important role in the physical experiment to analyze springback.

3. Design new anti-buckling fixture for cyclic testing

To successfully develop the fixture for anti-buckling of cyclic testing, three requirements are necessary. One requirement is that the whole part during a continuous tensile-compressive process should be covered for avoiding buckling. The other one is that the automatic alignment during a tensile-compressive process needs to be realized in order to solve the misalignment leading to reductions in the attainable compressive strain range before buckling. Lastly, side force and frictional force should be measured and controlled.

In this study, a new anti-buckling fixture was designed that enables cyclic testing of sheet metal specimens without buckling. Four acrylic wedge plates were used to entirely cover and clamp the specimen front surface in the initial position as shown in *Figure 4*.

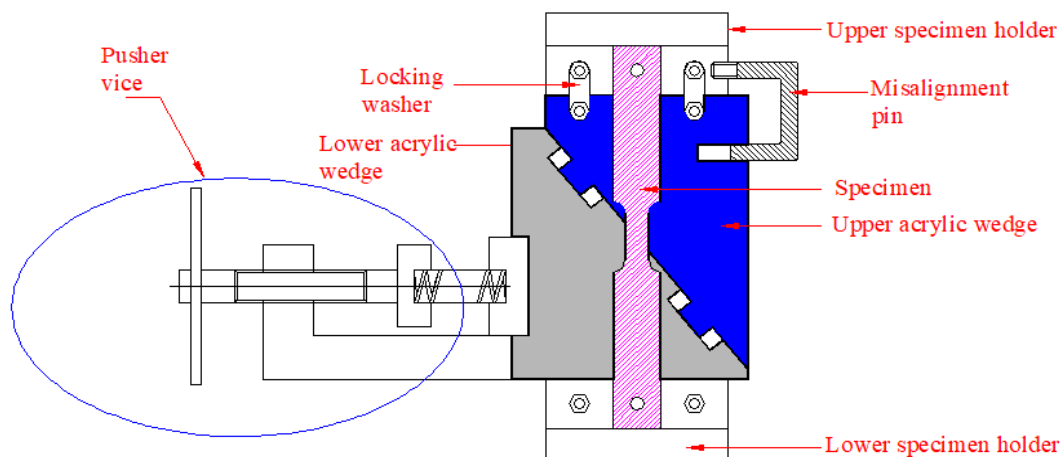


Figure 4. Detail description of newly design fixture at initial position

The acrylic block is a transparent material. It allows transferring of all visible light and has a greater level of optical clarity. It is also machinable and polishable. Therefore, there are possibilities to apply the digital image correlation (DIC) system to measure the strain.

During tension, both upper acrylic wedges and upper specimen holders are fixed by an extended locking washer and dragged up together. The key machined on the wedge surface of the upper acrylic block does not miss mating with the pocket machined on the wedge surface of the lower acrylic block. The pusher vice with a compressed spring attached on the left side of the lower acrylic block would generate side force to make the horizontal sliding movement of the lower block and keep the alignment of both blocks. The main body of the pusher vice is fixed with the table of the universal testing machine. Therefore, during tension two important linear movements should be considered, the positive Y-axis of the upper acrylic block and the positive X-axis of the lower acrylic block as shown in *Figure 5*.

During compression, unlock the extended locking washer and allow sliding down to upper blocks inclinedly on the wedge surface of the block. During this time lower acrylic wedges would be fixed from any moment. To prevent the fail-down of upper acrylic wedges by gravitational load, an additional two U shape misalignment pin was designed. It has a threaded end to fasten with the left side of the machine specimen holder and the unthreaded end will mate with the pocket machine on the left side of the upper acrylic blocks. The 3D assembly model of the newly designed anti-buckling fixture is shown in *Figure 6*.

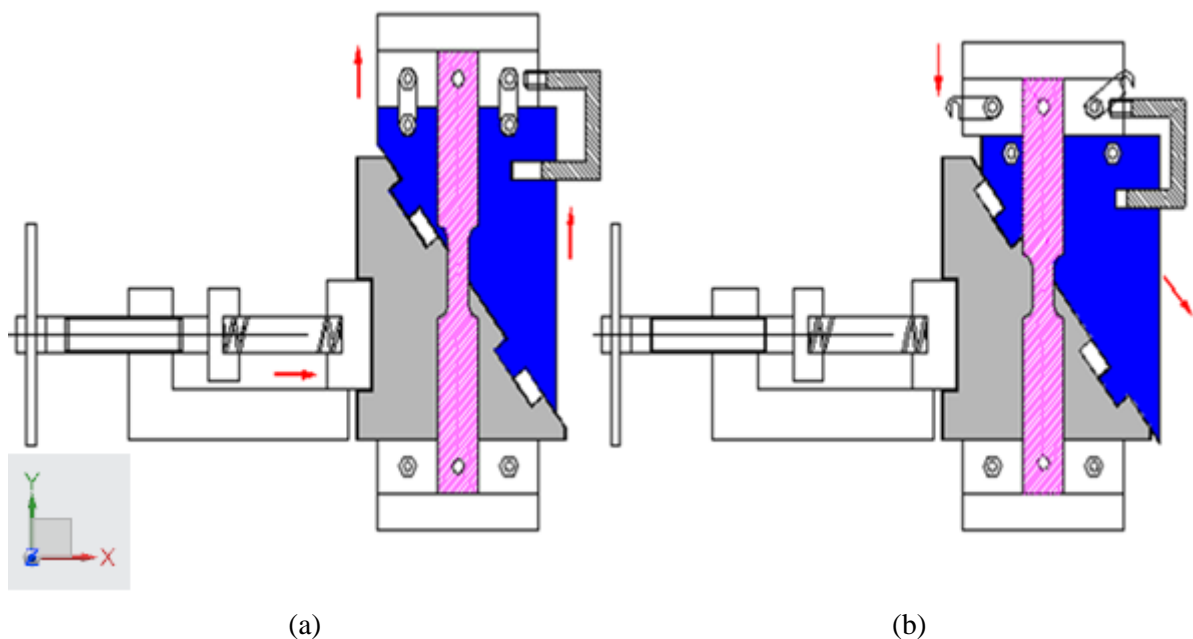


Figure 5. Direction of movement during testing: (a) during tension, (b) during compression

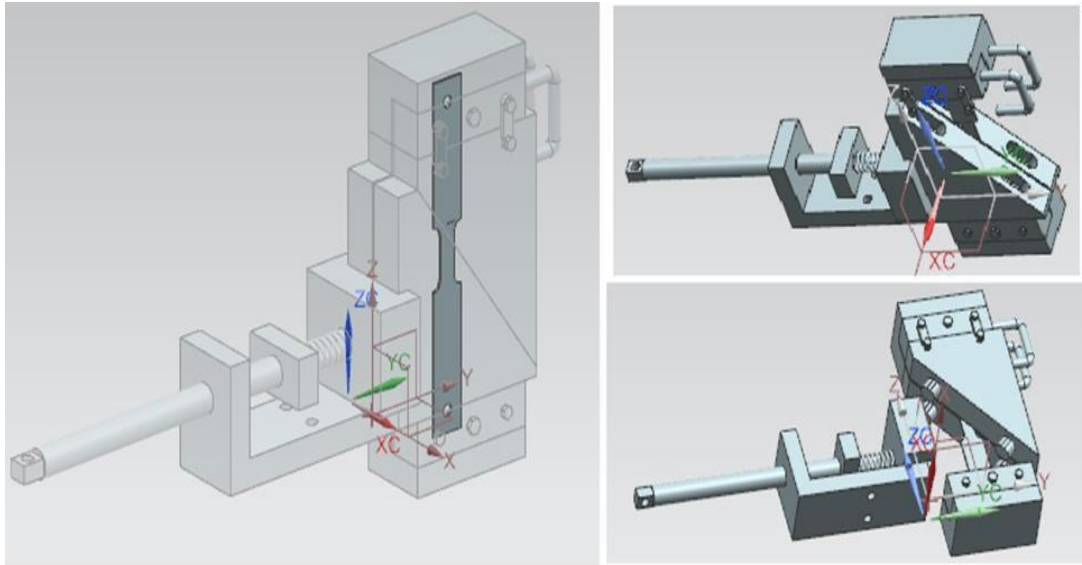


Figure 6. Assembly model of newly design fixture

Moreover, the device is integrated with DIC for full-field strain measurements within the test specimen. The DIC would be fully integrated with the universal tensile machine and record the strain distribution on the front surface of the specimen.

3.1. Special features of the new design

During cycle testing of sheet metal, the front surface of the specimen was completely covered and clamped using four acrylic wedge plates. The acrylic block has superior optical clarity and is clear, allowing the transfer of all visible light. Upper wedge blocks and upper specimen holders are fixed by an extended locking washer and pulled up together when tension force is applied. All upper wedge blocks would slide down on the wedge surface of the block during compression if the extended locking washer was unlocked. All lower wedge blocks would be fixed at any time throughout this period. The side alignment pin could stop the block from collapsing under the force of gravity. Because of the transparent property of acrylic blocks, there is a chance to use the DIC technique to quantify strain. In this new device no need of calculating supplementary forces related to the uniaxial direction and be free from misalignment problems.

4. Summary

To predict springback during cold stamping of sheet metal, designing and developing new anti-buckling apparatuses that particularly enable accurate tension-compression testing is mandatory. Because the supporting block material is transparent, the front surface of the specimen is fully visible and has the opportunity to use the DIC system to measure strain. In this newly designed fixture, no misalignment problem and no need of calculating the supplementary forces (tension/compression load for springs, side, and frictional forces) which directly affect the isotropic and kinematic behavior of the material. It is also simple, flexible, and suitable for any universal tensile testing machine. Upcoming challenges in

this device are still need controlling of friction between specimen and wedge blocks. Frequently polishing of acrylic block is also required to increase the optical visibility of the acrylic block making it easy and accurate strain measurement using a DIC system.

References

- [1] Agha, A., & Abu-Farha, F. (2022). Advanced anti-buckling device coupled with real-time digital image correlation for complex cyclic tension-compression testing of lightweight materials. *Journal of ASTM International*.
- [2] Choi, Y., Lee, J., Panicker, S. S., Jin, H. K., Panda, S. K., & Lee, M. G. (2020). Mechanical properties, springback, and formability of W-temper and peak aged 7075 aluminum alloy sheets: Experiments and modeling. *International Journal of Mechanical Sciences*, 170, p. 105344. <https://doi.org/10.1016/j.ijmecsci.2019.105344>
- [3] Wagoner, R. H., Lim, H., & Lee, M. G. (2013). Advanced issues in springback. *International Journal of Plasticity*, 45, pp. 3–20. <https://doi.org/10.1016/j.ijplas.2012.08.006>
- [4] Nanu, N., & Brabie, G. (2012). Analytical model for prediction of springback parameters in the case of U stretch–bending process as a function of stresses distribution in the sheet thickness. *International Journal of Mechanical Sciences*, 64 (1), pp. 11–21. <https://doi.org/10.1016/j.ijmecsci.2012.08.007>
- [5] Uemori, T., Okada, T., & Yoshida, F. (1998). Simulation of springback in V-bending process by elasto-plastic finite element method with consideration of Bauschinger effect. *Metals and Materials*, 4 (3), pp. 311–314. <https://doi.org/10.1007/BF03187783>
- [6] Yoshida, F., Uemori, T., & Fujiwara, K. (2002). Elastic–plastic behavior of steel sheets under in-plane cyclic tension–compression at large strain. *International Journal of Plasticity*, 18 (5–6), pp. 633–659. [https://doi.org/10.1016/S0749-6419\(01\)00049-3](https://doi.org/10.1016/S0749-6419(01)00049-3)
- [7] Cao, J., Lee, W., Cheng, H. S., Seniw, M., Wang, H. P., & Chung, K. (2009). Experimental and numerical investigation of combined isotropic-kinematic hardening behavior of sheet metals. *International Journal of Plasticity*, 25 (5), pp. 942–972. <https://doi.org/10.1016/j.ijplas.2008.04.007>
- [8] Härtel, M., Illgen, C., & Wagner, M. F. (2016, March). Experimental evaluation of Bauschinger effects during tension-compression in-plane deformation of sheet materials. IOP Conference Series: Materials Science and Engineering, Vol. 118, No. 1, p. 012018. <https://doi.org/10.1088/1757-899X/118/1/012018>
- [9] Chang, Y., Wang, B. T., Li, X. D., Wang, C. Y., Zhao, K. M., & Dong, H. (2020). A new continuous tensile-compressive testing device with friction-counteracting and anti-buckling supporting mechanism for large strain. *Journal of Materials Processing Technology*, 278, p. 116540. <https://doi.org/10.1016/j.jmatprotec.2019.116540>
- [10] Tisza, M., and Lukács, Z.: *Modelling and experimental investigation of large-strain cyclic plastic deformation of high strength dual-phase steels*, 2014 11th World Congress on Computational Mechanics.
- [11] Yoshida, F., & Uemori, T. (2002). A model of large-strain cyclic plasticity describing the Bauschinger effect and workhardening stagnation. *International Journal of Plasticity*, 18 (5–6), pp. 661–686. [https://doi.org/10.1016/S0749-6419\(01\)00050-X](https://doi.org/10.1016/S0749-6419(01)00050-X)